Applied Energy 181 (2016) 575–585

Contents lists available at ScienceDirect

Applied Energy

journal homepage: www.elsevier.com/locate/apenergy

Experimental investigation of a ground-coupled desiccant assisted air conditioning system

Arne Speerforck *, Gerhard Schmitz

Hamburg University of Technology, Institute of Engineering Thermodynamics, Denickestr. 17, 21073 Hamburg, Germany

HIGHLIGHTS

- A ground-coupled desiccant assisted air conditioning system is evaluated experimentally.
- The evaluation is carried out for steady state operation and the cooling period as a whole.
- The suitability of the system to provide comfort conditions is examined demonstrated.
- Energy comparisons with other air-conditioning systems are performed.
- The performance of the borehole heat exchangers for cooling is evaluated.

ARTICLE INFO

Article history:
Received 26 February 2016
Received in revised form 5 August 2016
Accepted 6 August 2016
Available online 31 August 2016

Keywords:
Desiccant wheel
Air conditioning
Borehole heat exchanger
Experimental

ABSTRACT

In a pilot installation at Hamburg University of Technology the coupled operation of an open cycle desiccant assisted air conditioning system with borehole heat exchangers is investigated. The paper presents experimental data recorded during the cooling period 2014. Results show that the electricity demand of the system can be reduced to the parasitic consumption of the fans, wheels and pumps. An electric energy efficiency ratio of 6.63 is achieved, enabling electricity savings of more than 70% compared to a conventional reference system and 54% compared to a desiccant assisted hybrid system relying on an electric chiller. Comfort conditions can be maintained during the whole cooling period. The borehole heat exchangers work highly efficient, exhibiting a seasonal performance factor of 192.

1. Introduction

The building sector is responsible for one third of the global final energy demand [1]. Even though demand for space heating is currently more important than the respective demand for space cooling, a considerable increase in cooling demand is expected due to climate change and income growth in regions with high cooling requirements. According to [2], the final energy demand for air conditioning is expected to be 40 times larger in the year 2100 than it was in the year 2000 and that it will exceed heating demand by 2060. Even for temperate climates a considerable increase is expected. By 2025, the installed cooling capacity in the European market is likely to be 55–60% higher than in 2010 [3]. This increasing demand is seen as one of the prime concerns in energy research [4].

Moisture removal accounts for a significant fraction of the mentioned air conditioning loads during the summer period. In a conventional system the air is cooled below the dew point temperature (e.g. 10 °C) to remove latent loads. Dehumidification causes large cooling capacities which are usually provided by an electric motor-driven vapour compression, causing a high demand for electricity. Therefore, efficient HVAC alternatives are important to lower greenhouse gas emissions related to electricity generation. In an open cycle desiccant assisted air conditioning system dehumidification and cooling can be separated within the process. First, moist air is dehumidified by means of a solid or liquid desiccant. Afterwards, the dried air can be cooled by a heat sink working at a higher temperature level (16 °C). This enables the usage of renewable heat sinks as for example shallow geothermal energy. While thermal energy is required for the regeneration of the desiccant, the required cooling capacity of the cold water cycle is reduced significantly.

These advantages are well established in literature [5]. Accordingly, a considerable amount of research has been conducted studying the design and performance of desiccant wheels either experimentally (e.g. [6–8]) or numerically (e.g. [9–12]). Furthermore, researchers have developed different system configurations

* Corresponding author.
E-mail addresses: arne.speerforck@tuhh.de (A. Speerforck), schmitz@tuhh.de (G. Schmitz).

http://dx.doi.org/10.1016/j.apenergy.2016.08.036
0306-2619/

Nomenclature

COP	coefficient of performance (–)
EER	energy efficiency ratio (–)
EB	energy balance (–)
f	primary energy factor (–)
h	enthalpy (kJ/kg)
MPF	monthly performance factor (–)
MMB	moisture mass balance (–)
P	electrical power (kW)
p	pressure (Pa)
Q	thermal energy (J)
$\dot{Q}$	thermal power (W)
SPF	seasonal performance factor (–)
T	temperature (°C)
t	time (s)
$\dot{V}$	volume flow (m^3/h)
W	electrical energy (J)
w	air humidity ratio (g/kg)
Δ	difference (–)
δ	relative difference (–)
λ	thermal conductivity (W/mK)
φ	relative humidity (%)

Subscripts

AC	air cooler
AH	air heater
AHU	air handling unit
aux	auxiliary
BHX	borehole heat exchanger
C	cooling
DW	desiccant wheel
el	electrical
eta	extract air
G	gas
HRW	heat recovery wheel
in	inlet
m	month
out	outlet
p	period
PE	primary energy
sup	supply air
th	thermal
v	vaporization
w	water

for different climate zones, overviews are provided in [4,13–17]. These systems can be divided in DEC (Desiccant Evaporative Cooling) systems which over dehumidify the air before it is cooled by water injection and hybrid systems which utilize a closed cooling cycle instead of water injection [13].

Several different hybrid systems have been proposed and were proven to be advantageous (e.g. [18–23]). While most of the systems rely on vapour compression chillers, further heat sinks are enabled through the possible increase of the required cold water temperature. Thermally driven adsorption chillers achieve their best performance for higher temperature levels of the cold water cycle and the thermal energy required to run the chiller can be supplied on similar temperature levels as the energy required for regeneration of the desiccant wheel. Fong et al. [24] proposed and simulated the coupling of a desiccant assisted air handling unit to a closed cycle adsorption chiller. In [25] such a system was investigated experimentally. The study showed that considerable primary energy savings are possible depending on the heat generation processes. Another alternative heat sink enabled through the desiccant wheel is shallow geothermal energy. However, just a few papers have investigated this combination so far. El-Agouz and Kabeel [26] modelled and simulated the integration of a geothermal heat sink in a DEC system in order to precool the air before humidification. They provided system COPs for different ambient conditions and showed that the geothermal heat sink enabled the system to provide better comfort conditions and decrease the supply air temperature. A maximum COP of 1.03 was reported for the presented configuration. They assumed a constant outlet temperature of the geothermal system of 20 °C, seasonal increasing soil temperature through heat rejection during the cooling period was not considered in their study. A similar system configuration is investigated by Enteria et al. [27], who simulate an alternative energy system for a single family detached house in Japan. A U-tube ground heat exchanger of 10 m depth is used in order to support a DEC system. They report that utilization of the low grade geothermal energy benefits the system as it reduces the supply air temperature even during the hottest days of the year. However, details about the ground heat exchanger and its exact contribution to the system are not discussed. The investigation of Khalajzadeh et al. [28] did not incorporate air dehumidification through a desiccant wheel. The combination of an indirect evaporative cooling coil and a ground circuit consisting of four borehole heat exchangers (BHXs) was evaluated. The authors simulated their circle for ambient air and soil conditions representing a chosen day in Theran. The presented system was able to provide comfort conditions in a more efficient way than indirect evaporative cooling alone. The study of Angrisani et al. [29] investigates the coupling of a desiccant assisted air handling unit to a geothermal well of 94 m depth, which is used for heat generation. The heat is used to regenerate the desiccant wheel and drive an absorption chiller for cooling purposes; additionally hot water for domestic use is generated. They found that depending on the actual utilization of domestic hot water primary energy savings of up to 90% can be achieved compared to a conventional reference system. Schmitz and Casas [30] investigated a hybrid system utilizing BHXs for direct cooling. A small cogeneration engine was used for heat generation, the performance of the air handling unit alone was evaluated experimentally and possible primary energy savings of 60% were identified for one stationary point. Radiant cooling and parasitic energy consumption was not taken into account, the air conditioing system as a whole was not evaluated. Details regarding the supply of heat, cold or electricity are not presented by the authors. The presented figures also reveal shortcomings regarding mass and energy balances of the diffferent components of the air handling unit including the desiccant wheel, making results less reliable. The authors reported that the system might not be able to maintain comfort conditions during the whole cooling period, details about the geothermal heat sink and potential seasonal warming of the soil were not presented.

Even though the coupling of BHXs for direct cooling to a desiccant assisted air conditioning system has been identified as an efficient alternative to conventional systems, the literature lacks comprehensive studies of this system configuration. To the author's knowledge no study so far provided a detailed experimental analysis of such a system evaluating its performance for a longer cooling period with varying ambient conditions and taking parasitic energy consumption into account. Performance indicators as latent, thermal or electric COPs have not been presented so far. These quantities however are important to evaluate and compare different system configurations. To increase reliability, energy and water balances for the different components of the air handling unit are presented with the respective quantities.

Furthermore, the existing studies do not provide details about the configuration and efficiency of the geothermal heat sink. Cold water temperature levels and seasonal warming of the soil are not taken into consideration. This paper aims to address these gaps in literature. A novel test facility which combines a desiccant assisted air handling unit, cooling ceilings and BHXs is investigated experimentally. Through the cooling ceilings ventilation and sensible cooling can be separated and the mass flow of the supply air can be chosen just high enough to achieve an acceptable indoor air quality, minimizing the energy consumption of the fans [31,32]. Furthermore, in combination with BHXs, the cooling ceilings can be used to increase the cold water temperature, so that comfort conditions in the room can be maintained during the whole cooling season. The system is designed to be an efficient alternative for air conditioning systems in temperate climate. It is evaluated for the summer period of 2014. It is compared to reference systems relying on vapour compression chillers, special attention is paid to the performance of the BHXs.

2. Test facility

The test facility shown in Fig. 1 is located at Hamburg University of Technology and consists of eight 20 ft containers. The four containers at the ground level contain the air handling unit as well as the further technical installations. The upper four containers serve as office room with an area of 54 m^2 and are used as reference for the air conditioning system.

2.1. System description

The layout of the pilot installation is shown in Fig. 2. It can be divided into three major parts: the air-handling unit, the hot and cold water circuit, and the reference room.

The air-handling unit is designed as a hybrid system, similar to the facility presented in [25]. The outdoor air is dehumidified in a desiccant wheel (1–2) and precooled by the sensible heat regenerator (2–3). Both wheels exhibit a diameter of 0.6 m, lithium

Fig. 1. Test facility, air handling unit and BHX.

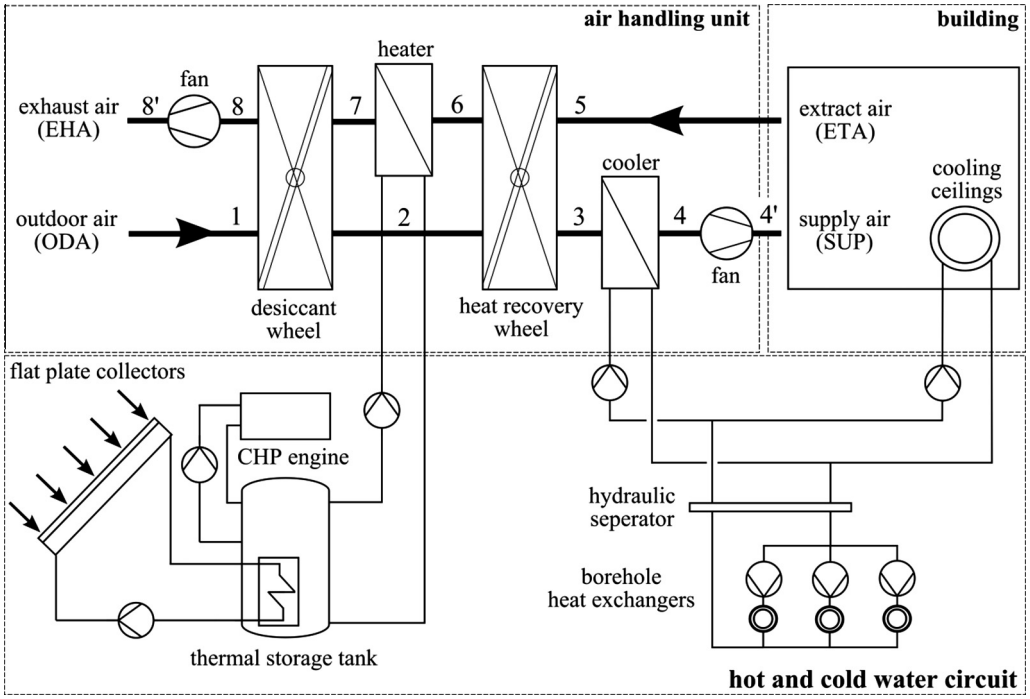

Fig. 2. Layout of the pilot installation.

chloride is used as desiccant. The air is then cooled down by a water to air heat exchanger (3–4) to achieve the desired supply air temperature. The extract air is preheated by a heat recovery wheel (5–6) before it is heated further to the required regeneration temperature (6–7). The air finally regenerates the desiccant wheel (7–8) before it exits the installation. In comparison to a conventional air conditioning unit, the usage of a desiccant wheel to separate dehumidification and cooling reduces the cooling load and enables the coupling of heat sinks above the dew point temperature (e.g. BHXs) to the air handling unit [31].

The cold water required in the air cooler and the cooling ceilings can be generated by three double U-tube BHXs, each of them exhibiting a depth of 80 m. A hydraulic separator is used to connect them to the coils. Just two of the three BHXs were utilized for this study. Due to the comparatively large thermal capacity of the soil, a storage tank is not used on the cold water side. The hot water necessary for regeneration of the desiccant wheel is provided by a small scale CHP engine (nominal data: $P_{el} = 5$ kW, $\dot{Q}_{th} = 12.5$ kW) and a 20 m^2 flat plate solar thermal system. Heat supply and demand is decoupled by using a 1 m^3 stratified thermal storage tank. The heat transfer fluid within the hot and cold water circuit is a mix of water and ethylene glycol (21 vol.%).

2.2. Measurement devices and data acquisition

In order to investigate the transport and conversion of energy within the system, the usage of adequate measurement devices is crucial. To evaluate the air handling unit and the connected reference room, temperature and humidity are measured at all stages within the air handling unit marked with numbers in Fig. 2. To account for the inhomogeneity of temperature and humidity within the air stream, flow averaging is utilized as proposed by [33]. The volume flow is measured at positions 4 and 8. Pressure drops are measured across all components of the air handling unit. The cold and hot water loops are evaluated by one volume flow measurement and two temperature measurements per component. Furthermore, the electricity demand of all devices connected to the grid is measured. Table 1 shows the selected types of sensors and their respective uncertainties.

The volume flow of air is determined by comparing the static pressure in front of the fan's inlet ring with the static pressure measured in the narrowest point of the inlet ring. A calibrated nozzle factor is provided by the manufacturer. To increase the quality of this measurement and check the factor provided by the manufacturer, an onside calibration with an orifice plate measurement according to DIN EN ISO 5167-2 [34] has been conducted. Relative humidity of the air is measured using capacitive sensors, which are usually subjected to a drift and can cause high inaccuracies in the evaluation of air conditioning systems. To take care of those effects, all sensors used in the following analyses have been calibrated at eight different values of relative humidity for four different temperatures, using a dew point sensor as reference. The correction of each measured value is then achieved by a linear interpolation between the respective 32 values. Due to the drift of the humidity sensors, this procedure is repeated on a yearly basis. The calibration procedure for this study has been conducted in April 2014. Furthermore, to ensure a reliable evaluation of the BHXs as well as the further heat exchangers the Pt100 temperature sensors were checked in a reference bath. Each two of them exhibiting similar characteristics were used for measurements in one loop. Due to the small occurring temperature differences, especially in the BHXs, an accurate temperature measurement is crucial to obtain adequate data for the system and component evaluation. Soil temperature is measured at eight different locations in the boreholes using thermistor strings. All measured data of the air handling unit and the hydraulic cycles are recorded every 60 s.

3. Monitoring results

This study is based on measured data for the months June, July, August and September 2014. The system as a whole is evaluated in two steps. First, to provide a deeper understanding of the system configuration, measured data for steady state operation are presented. In the second step the whole system is evaluated by comparing its heat and electricity demand to the respective demands of two different reference systems. This comparison is based on recorded data of 24 days of the investigated period. Heat sources of the pilot plant are not taken into consideration. Heat for regeneration of the desiccant wheel and electricity are considered as inputs to drive the air conditioning system. Finally, the efficiency of the BHXs is evaluated.

3.1. Steady state operation

All data presented in this section were recorded on June 10th at 9:02 pm. Fig. 3 shows the state changes within the air handling unit for a supply air flow of $\dot{V}_{sup} = 937$ m^3/h. Extract and supply air volume flows are controlled to be equal. Furthermore, chosen energy and mass balances are presented: MMB_{AHU} marks the moisture mass balance for the air handling unit, EB_{HRW}, EB_{DW}, EB_{AC}, EB_{AH} mark energy balances for the heat recovery wheel, the desiccant wheel, the air cooler as well as the regeneration air heater. All quantities are presented with their deduced uncertainty according to the measurement equipment presented in Table 1. Error propagation is calculated according to [35], an example is provided in [36].

$$\begin{aligned} MMB_{AHU} &= \frac{\dot{m}_{sup}\cdot(w_1 - w'_4)}{\dot{m}_{eta}\cdot(w'_8 - w_5)} \quad EB_{HRW} = \frac{\dot{m}_{sup}\cdot(h_3 - h_2)}{\dot{m}_{eta}\cdot(h_5 - h_6)} \\ EB_{DW} &= \frac{\dot{m}_{sup}\cdot(h_2 - h_1)}{\dot{m}_{eta}\cdot(h_7 - h_8)} \\ EB_{AC} &= \frac{\dot{m}_{sup}\cdot(h_4 - h_3)}{\dot{m}_{w,AC}\cdot(h_{in} - h_{out})} \quad EB_{AH} = \frac{\dot{m}_{eta}\cdot(h_7 - h_6)}{\dot{m}_{w,AH}\cdot(h_{in} - h_{out})} \end{aligned} \tag{1}$$

The numbers of the state changes in the presented equations as well as in Fig. 3 refer to Fig. 2. For major clarity states behind the fans (4′ and 8′) are not included in Fig. 3, as both are very close to the respective states in front of the fan. The denominators of

Table 1
Measurement devices used in the pilot plant.

Measured property	Sensor type or principle	Uncertainty
Air and water temp., T	Resistance thermometer, Pt100	$\pm 1/3\cdot(0.3 + 0.005\cdot T)$
Soil temperature, T	Thermistor string	±0.5 °C
Relative humidity, φ	Capacitive humidity sensor	±2% r.h. for 10% < φ < 90%
Volume flow (air), $\dot{V}$	Differential pressure	±10%
Volume flow (water), $\dot{V}$	Electromagnetic flow meter	±0.5% ± 1 mm/s
Electric energy, W	AC energy meter	±2%
Pressure difference, Δp	Ceramic fulcrum lever tech.	±2% FS, (range: 0–300 Pa & 0–1000 Pa)

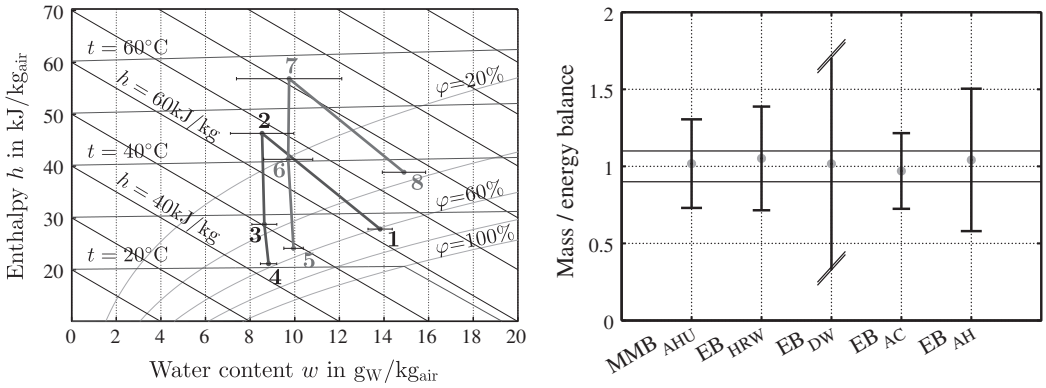

Fig. 3. State changes during the air conditioning process (left) and energy and mass balances (right).

EB_{AC} and EB_{AH} describe water state changes of the water air heat exchangers. All presented balances exhibit a deviation smaller than 5%, indicating that steady stated operation was reached and the measured data are valid. The uncertainties of the measurement devices reported in Table 1 lead to significant deduced uncertainties for the investigated quantities. The uncertainty of EB_{DW} cannot even be displayed on the chosen axes, which is due to the small changes of enthalpy occurring in the desiccant wheel. However, the accurate fit of the different balances underlines that the calibration procedure is suitable and the measured data are trustworthy. Considering the whole cooling period, all balances were usually met within a deviation of smaller than 10% on a daily basis. The state changes of the air displayed in Fig. 3 are explained in Section 2.1. A slight change of water content can be observed for the air stream passing the cooler (3–4). This can be caused by seal leakage and carryover at the heat recovery wheel and the associated mixing effect of room and supply air. The slight moisture decrease from 5 to 6 might result from the same cause. However, taking measurement uncertainties into account, slight differences in water content can hardly be interpreted. Rotational speed of the wheels was set constant during all measurements, detailed wheel parameters are presented in Table 4. Table 2 provides information regarding the different water based heat exchangers.

The plant can usually be operated with cold water temperatures above 17 °C. Given this temperature level, the cooling power required by the air cooler and the cooling ceilings can be fully provided by just one BHX. Due to constructional reasons the BHXs have been drilled roughly 30 m away from the test facility. Therefore, the occurring deviation of 8% between the heat flow rejected through the BHX and the heat transferred through the air cooler as well as the cooling ceilings might be due to occurring losses to the environment. However, the occurring deviation could fully be caused by measurement uncertainties, according to Table 2. Different performance measures have been defined in literature in order to evaluate a desiccant assisted air handling unit (e.g. [14,22]). The COPs used in this study are presented in Eq. (2). To include air leakage the respective quantities are evaluated for the air handling unit as a whole. The results for the investigated point of time are presented in Table 3.

Table 2
Heat and mass fluxes as well as inlet and outlet temperatures of the different heat exchangers.

	$\dot{Q}$ (kW_{th})	T_{in} (°C)	T_{out} (°C)	$\dot{m}$ (kg/min)
Air heater	4.6 ± 0.2	66.3 ± 0.2	51.9 ± 0.2	4.7 ± 0.1
Air cooler	2.4 ± 0.2	17.8 ± 0.1	20.7 ± 0.1	12.4 ± 0.2
Cooling ceilings	1.4 ± 0.1	18.0 ± 0.1	21.3 ± 0.1	4.7 ± 0.1
BHX1	4.1 ± 0.3	21.1 ± 0.1	17.5 ± 0.1	17.2 ± 0.4

$$\mathrm{COP}_{lat} = \frac{\dot{m}_{sup} \cdot (w_1 - w_{4'}) \cdot \Delta h_v}{\dot{m}_{w,AH} \cdot (h_{in} - h_{out})} \quad \mathrm{COP}_{th} = \frac{\dot{Q}_c}{\dot{m}_{w,AH} \cdot (h_{in} - h_{out})}$$
$$\mathrm{COP}_{th,aux} = \frac{\dot{Q}_c}{\dot{m}_{w,AH} \cdot (h_{in} - h_{out}) + P_{el}} \quad \mathrm{COP}_{el} = \frac{\dot{Q}_c}{P_{el}} \tag{2}$$

The cooling power $\dot{Q}_c$ can be defined for the air handling unit

$$\dot{Q}_{c,AHU} = \dot{m}_{sup} \cdot (h_1 - h_{4'}) \tag{3}$$

and the system as whole, taking the cooling ceilings into account.

$$\dot{Q}_{c,Sys} = \dot{m}_{sup} \cdot (h_1 - h_{4'}) + \dot{m}_{w,CC} \cdot (h_{in} - h_{out}) \tag{4}$$

COP_{lat} relates the latent heat difference of the supply air to the energy transferred as heat through the regeneration air heater. The measured value of 0.84 marks an acceptable efficient dehumidification process of the investigated air handling unit for the presented boundary conditions. The thermal COP_{th} compares the cooling power of the supply air to energy required for regeneration, whereas the $\mathrm{COP}_{th,aux}$ also includes the auxiliary electric power required to run the AHU. The measured values both excess unity, indicating an efficient process. Regarding the definition of $\mathrm{COP}_{th,aux}$ it needs to be mentioned that in the denominator electricity and thermal energy are simply summed up, even though both types of energies are of different thermodynamic value. However, the value is provided here for comparability. The electric $\mathrm{COP}_{el} = 9.14 \pm 1.15$ marks the main strength of the hybrid system. As a renewable heat sink is combined with desiccant cooling, the electricity consumption is reduced to the parasitic energies required to power the fans, pumps and wheels. However, these energy fluxes cannot be neglected in the evaluation of the system. The overall power required to run the plant sums up to 762 W, as displayed in Fig. 4.

3.2. Period evaluation of the system performance

The period evaluation of the system is based on recorded data of 24 days of June (3), July (16), August (3) and September (2) 2014. During the chosen days the system was operated in dehumidification mode between 7 am and 10 pm. Measurements for each day were conducted 24 h, in order to take the standby consumption into account. Table 5 provides information about ambient, supply

Table 3
Chosen COPs evaluated for steady state operation.

	COP_{lat}	COP_{th}	$\mathrm{COP}_{th,aux}$	COP_{el}
Air handling unit	0.84 ± 0.14	1.2 ± 0.17	1.03 ± 0.14	7.27 ± 1
Whole system	0.84 ± 0.14	1.5 ± 0.19	1.29 ± 0.16	9.14 ± 1.15

Table 4
Parameters of the desiccant and the heat wheel.

	Desiccant wheel	Heat recovery wheel
Diameter	0.6 m	0.6 m
Length	0.25 m	0.25 m
Specific surface	2722 m^2/m^3	2914 m^2/m^3
Desiccant	LiCl	–
Matrix material	Cellulose	Aluminium
Channel type	Sinusoidal	Sinusoidal
Channel height	1.8 mm	1.6 mm
Channel width	3.8 mm	3.9 mm
Rotational speed	16 rph	248 rph

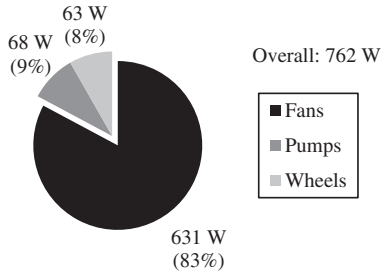

Fig. 4. Electricity demand of different components and the test facility as a whole.

air and room conditions for the evaluated days. All quantities are averaged over the daily operation time of the air conditioning system.

The measured states of the ambient and room air during the considered days, as well as the comfort zones defined in DIN EN ISO 15251 [37] are plotted in Fig. 5. The first hour of system operation is not considered here, in order to exclude start up effects. The comfort zones were defined to ensure less than 6% (Cat. I) or 10% (Cat. II) of people being dissatisfied with the indoor conditions. According to Fig. 5 the air conditioning system satisfied the requirements of category I for 80% of the investigated period, while a climate of category II could be maintained for 99% of the time. The temperature level of the reference room did not exceed comfort requirements during any time, which indicates that seasonal warming of the soil surrounding the BHX did not significantly influence the capabilities of the system to ensure comfort climate. The deviations occur due to an increase in relative humidity, they are mainly caused by limiting the regeneration temperature of the desiccant wheel to 60 °C and internal latent loads of the room. However, taking the small percentage of deviations into account, the presented system is well capable to ensure comfortable indoor conditions. Table 6 presents the Energy Efficiency Ratios (EERs) of the system, evaluated for the whole period. The values are derived similar to the COPs defined in Eq. (2). The respective terms in the nominators and denominators are integrated over all days considered in this study:

$$\mathrm{EER}_{\mathrm{lat,p}} = \frac{\int_{\mathrm{p}} \dot{m}_{\mathrm{sup}} \cdot (w_1 - w_{4'}) \cdot \Delta h_{\mathrm{v}} \mathrm{d}t}{\int_{\mathrm{p}} \dot{m}_{\mathrm{w,AH}} \cdot (h_{\mathrm{in}} - h_{\mathrm{out}}) \mathrm{d}t} \quad \mathrm{EER}_{\mathrm{th,p}} = \frac{\int_{\mathrm{p}} \dot{Q}_{\mathrm{c}} \mathrm{d}t}{\int_{\mathrm{p}} \dot{m}_{\mathrm{w,AH}} \cdot (h_{\mathrm{in}} - h_{\mathrm{out}}) \mathrm{d}t}$$

$$\mathrm{EER}_{\mathrm{th,aux,p}} = \frac{\int_{\mathrm{p}} \dot{Q}_{\mathrm{c}} \mathrm{d}t}{\int_{\mathrm{p}} \{\dot{m}_{\mathrm{w,AH}} \cdot (h_{\mathrm{in}} - h_{\mathrm{out}}) + P_{\mathrm{el}}\} \mathrm{d}t} \quad \mathrm{EER}_{\mathrm{el,p}} = \frac{\int_{\mathrm{p}} \dot{Q}_{\mathrm{c}} \mathrm{d}t}{\int_{\mathrm{p}} P_{\mathrm{el}} \mathrm{d}t} \tag{5}$$

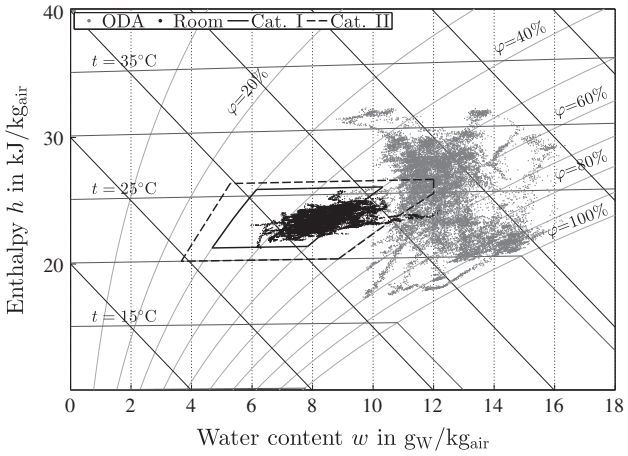

Fig. 5. Ambient and room air states during the investigated period.

Table 6
Chosen EERs evaluated for the investigated period.

	$\mathrm{EER}_{\mathrm{lat,p}}$	$\mathrm{EER}_{\mathrm{th,p}}$	$\mathrm{EER}_{\mathrm{th,aux,p}}$	$\mathrm{EER}_{\mathrm{el,p}}$
Air handling unit	0.9 ± 0.15	1.12 ± 0.17	0.92 ± 0.14	5.42 ± 0.82
Whole system	0.9 ± 0.15	1.35 ± 0.19	1.12 ± 0.16	6.63 ± 0.93

The presented integrals are evaluated numerically by multiplying the quantities with the chosen step size for data acquisition. The three EERs related to the thermal energy required for regeneration of the desiccant are of the same range as the COPs presented for the chosen steady state operation. They provide evidence that an efficient operation of the system can be maintained for the whole cooling season. As indicated above, the main achievement of the system is the high electric EER. Taking its definition according to Eq. (5) into account, the deviation between the steady state value (Table 3) and the value for the period as a whole (Table 6) can solely be explained by changes in the numerator. During the days considered here, the cooling load was in general smaller than for the steady state point presented above. The electricity consumption of the system remains fairly constant, independent of the cooling load.

To further evaluate the presented air conditioning system it is suitable to compare it to reference processes. In this study the pilot installation is compared to two different systems which are relying on vapour compression chillers to supply air coolers and cooling ceilings. The first reference system (DP-VC) is a conventional air conditioning system relying on dehumidification through condensation and a vapour compression chiller. The air handling unit of this system is shown in Fig. 6.

Key assumptions made regarding this process are:

- Supply air water content and mass flow rate: measured data of pilot installation,
- Supply air temperature: 16 °C,
- Energy Efficiency Ratio ($\mathrm{EER} = \frac{Q}{W}$) of the chiller, EER = 3. Q is the thermal energy transferred from the air to the cold water circuit in order to cool and dehumidify the air. W is the electric energy

Table 5
Boundary conditions for system evaluation.

$\emptyset T_{\mathrm{out}}$ (°C)	$\emptyset T_{\mathrm{sup}}$ (°C)	$\emptyset T_{\mathrm{room}}$ (°C)	$\emptyset w_{\mathrm{out}}$ (g_W/kg_{air})	$\emptyset w_{\mathrm{sup}}$ (g_W/kg_{air})	$\emptyset w_{\mathrm{room}}$ (g_W/kg_{air})	$\emptyset \dot{V}_{\mathrm{sup}}$ (m^3/h)
19.7–28.5	21.4–22.7	24.1–22.7	14.9–11.0	9.1–7.2	9.9–7.7	947–993

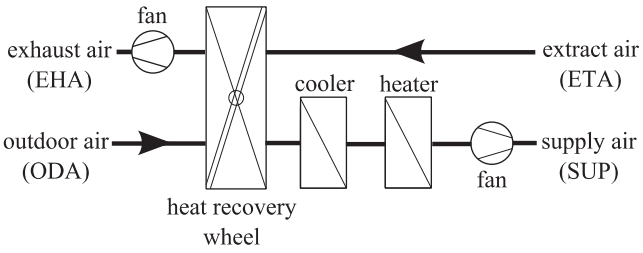

Fig. 6. Air handling unit of the reference system DP-VC.

required to operate the chiller, including a dry heat rejection process.

To ensure a fair comparison, EER is chosen slightly higher as recommended by [38]. Due to the lower supply air temperature level of the reference system the sensible load removed by the air stream increases. The respective difference is credited to the conventional process, in order to ensure a meaningful comparison. The parasitic energy consumption of the reference system is calculated based on measured data of the pilot plant. Furthermore, the lower electricity consumption of the fans due to the absence of the desiccant wheel and the regeneration heat exchanger is taken into account.

A hybrid air conditioning system relying on a vapour compression chiller is chosen as second reference (DW-VC). This process is defined through replacing the BHXs by a conventional chiller, while the rest of the investigated system remains unchanged. Basic assumptions regarding this reference system are:

- Supply air temperature, water content and mass flow rate: measured data of pilot installation,
- Electricity consumption of all components except the chiller: measured data of pilot installation,
- Energy Efficiency Ratio of the chiller including dry heat rejection, EER = 3.2.

The EER of the chiller is chosen slightly higher for the second reference system, in order to take the higher temperature level of the evaporator into account. To evaluate the whole investigated system, its energy demand in terms of electricity and heat is compared with the respective demands of the defined references. Fig. 7 shows the energy demands of the three systems summed up for the whole investigated period. To increase understandability, the results are divided by the number of investigated days (24). Standby consumptions of all electric components are included.

Regarding the electricity demand, 71% of the amount required to run the reference system based on dehumidification through condensation (DP-VC) can be saved by the pilot plant (DW-BHX). Compared to the hybrid system (DW-VC) electricity savings of 54% are achieved. While the chiller accounts for more than half of the overall amount of electricity consumed (79% and 54%) in the cases of both reference systems, the electricity consumption of the BHX's pumps accounts for just 2% of the demand of the test facility. This small share is hardly visible in Fig. 7 and even lower than the aggregated standby consumption (5%). The amount of energy as heat demanded by the pilot plant and the hybrid reference system (DW-VC) is 2.5 times higher than the amount required to run the conventional reference system (DP-VC), as the desiccant wheel needs to be regenerated. Note that quality of the energy as heat is not taken into account in this comparison. While the energy demand of the pilot plant is measured directly, the demand of the reference systems is calculated using the assumptions listed above. The respective quantities for the conventional reference system (DP-VC) depend on the supply air flow rate and humidity ratio, these measured values are subjected to higher uncertainties.

Table 7 presents more detailed information about the system performance under different ambient conditions. Electric and thermal EERs as well as achieved energy savings compared to the reference systems are presented for chosen days of the cooling period. The respective measurement uncertainties are not provided, as they are of similar magnitude as the above presented uncertainties for the respective quantities. During warmer days, as July 19 or July 20, the thermal efficiency ratio is maximised due to the higher

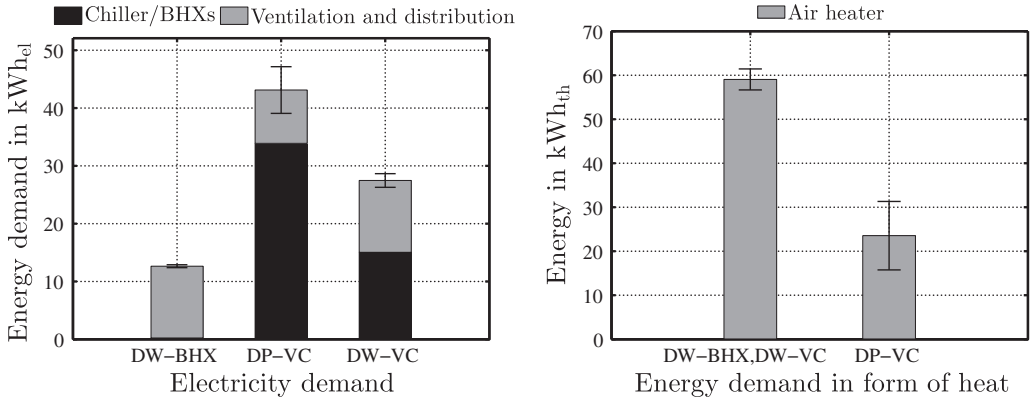

Fig. 7. Energy demands of the pilot plant (DW-BHX) and the reference systems (DP-VC, DW-VC).

Table 7
Chosen performance figures evaluated for different representative days of the cooling period.

	$\emptyset T_{out}$ (°C)	$\emptyset w_{out}$ (g_W/kg_{air})	$\emptyset w_{room}$ (g_W/kg_{air})	$\emptyset T_{room}$ (°C)	$EER_{th,d}$ (–)	$EER_{el,d}$ (–)	$\Delta_{el,DP-VC}$ (%)	$\Delta_{el,DW-VC}$ (%)	$\Delta_{Q,DP-VC}$ (%)
Jul 08	19.7	13.1	7.7	22.7	0.9	5.4	69.7	44.9	181.1
Jun 08	23.0	12.2	7.8	23.2	1.3	6.4	71.7	55.1	136.1
Jul 20	27.8	12.8	8.7	23.2	1.8	8.2	71.9	59.1	195.3
Jul 19	28.5	11	8.3	23.4	2.2	7.2	69.3	58.8	74.3
Jul 09	23.7	14.9	9.1	22.9	1.2	7.6	72.3	53.8	366.4

sensible load of the air conditioning unit. The efficiency is slightly higher for July 19 where the ambient humidity ratio is lower; the increased amount of heat required for regenerating the desiccant outweighs the effect of the increased latent load. The same effect explains the thermal efficiency for July 9, which is the day exhibiting the highest average outdoor humidity. During all of the mentioned days the electric EER is high, which can also be explained by the high load due to the ambient conditions. As mentioned above, the electric energy to drive the investigated system remains fairly constant, just slightly depending on the operating conditions. June 8 represents a typical summer day for the city of Hamburg with moderate temperatures and comparatively high latent loads. The same holds true for July 8 with even lower temperature and higher latent loads. Electric and thermal EERs are comparatively low for these days, due to the above mentioned reasons. The definition of both quantities might be misleading for the mentioned days as outside temperature is at least temporarily underneath the supply air temperature, while dehumidification is still necessary. However, the comparison to the reference systems reveals that the presented system is also efficient under these conditions, ensuring about 70% electricity savings compared to the conventional and 44–55% compared to the desiccant assisted reference system. The last column of the table marks the surplus of heat which is required to drive the desiccant assisted systems on comparison to the conventional system. The quantity is highly depending on the humidity ratio of the outside air.

From a primary energy perspective, the investigated system will in any case be superior to the hybrid reference system, as it exhibits a smaller electricity demand while heat demand is equal. Whether the presented system is superior to the conventional reference system depends on the efficiency of the energy conversion processes for heat and electricity supply, which usually vary highly among different locations. Considering the boundary conditions prevalent in Germany (Efficiency for electricity supply: $f_{p,el} = 2.4$ kW h_{PE}/kW h_{el}, and for natural gas supply: $f_{p,G} = 1.1$ kW h_{PE}/kW h_{Gas} [39]), the usage of a simple gas boiler ($\eta = 0.85$) combined with solar energy is evaluated in Fig. 8. The primary energy savings achieved through the investigated system during the whole cooling period in comparison to the reference systems are defined by the respective lines.

Compared to the conventional reference system (DP-VC), the exclusive usage of the gas boiler is sufficient to achieve primary energy savings of 21%. With increasing solar fraction these savings increase to 71%, which is equal to electricity savings. Compared to the desiccant assisted reference system (DW-VC) savings reach between 25% and 54%, depending on the solar fraction.

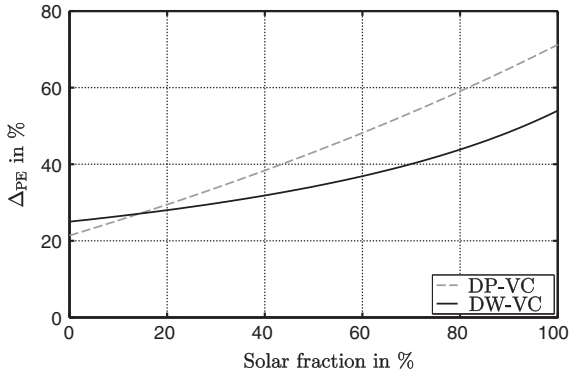

Fig. 8. Primary energy savings achieved through the investigated system.

3.3. The geothermal heat sink

The structure of the soil surrounding the three BHXs of the test facility is shown in Fig. 9. The first 18 m beyond the surface consist of medium and fine sand. Underneath the sand, a layer of mainly till and silt is prevalent. The biggest part of the BHXs is surrounded by micaceous clay which is located underneath 30 m (for BHX 1) or 32 m (for BHX3). Significant ground water flows do not occur. All three BHXs were drilled 80 m deep and built as double U-tube heat exchangers, as displayed in Fig. 9. To ensure thermal connection between the tubes and the soil, a grouting material with a thermal conductivity of $\lambda = 2$ W/mK is used inside the borehole. Thermistorstrings are utilized for temperature measurements. The respective temperatures are measured directly within the borehole right next to the double U-tube heat exchangers at 1, 5, 10, 15, 20, 40, 60, and 80 m below the surface.

While BHX 1 and BHX 3 were operated, BHX 2 was not utilized during the considered period. The distance of 17 m between the boreholes ensures that no interaction between them needs to be taken into account [40]. The temperature profile of the undisturbed soil next to BHX 2 is shown in Fig. 10 (left). While the soil temperature above 15 m is subject to changes during a year, the temperature below that point remains fairly constant at 9.6 °C (yearly average over 15, 20, 40, 60, and 80 m). This temperature level is almost equal to the mean yearly temperature for Hamburg of 9.7 °C, which is usually the case in the region of undisturbed soil [40]. This temperature level can efficiently be utilized for air conditioning processes which do not require condensation. However, as soon as the BHX is used, the temperature of the surrounding soil rises, as displayed in Fig. 10 (right) for BHX 3. The graph indicates the soil temperature averaged over the constant zone. The black line indicates the yearly average. After switching off the BHX,

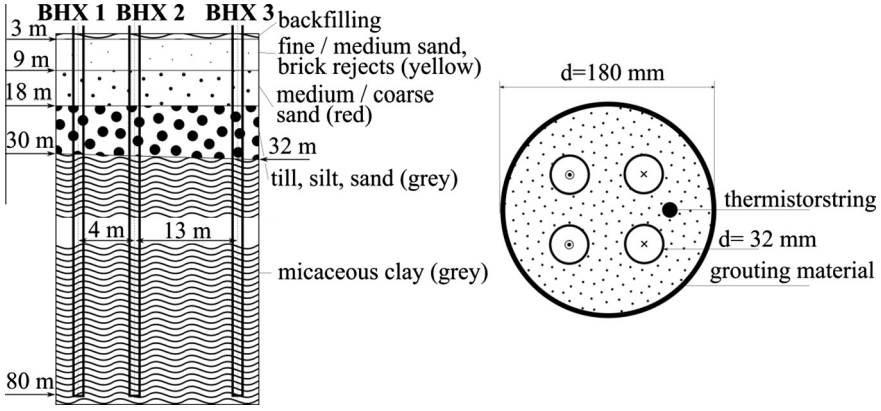

Fig. 9. Structure of the soil and the BHXs.

temperature declines rapidly. Despite that, during July (the hottest of the investigated months), the temperature level after decline over night remained 2 °C above the yearly average. The overall temperature increase is crucial to maintain comfort conditions for the cooled space and can be influenced by the number of BHXs utilized. The two BHXs operated for this study were sufficient to maintain comfort conditions during the whole investigated period. After the cooling period, temperature declines slowly to approach the yearly average.

At each point in time just one of the two BHXs is used and the respective pump is controlled to ensure that the mass flow through it equals the sum of the mass flows demanded by the cooling ceilings and the air cooler. If this flow rate is smaller than the minimum flow rate of the respective pump, it is operated at this minimum flow rate, which is the case for most of the timespan considered here. Fig. 11 visualizes the strategy applied to switch between the BHXs. The upper graph shows the cooling power demanded by the air cooler as well as the cooling ceilings and the amount provided by the BHXs during an exemplary day (August 2). The second graph displays the inlet temperature of the air cooler and the cooling ceilings as well as the outlet temperatures of the BHXs. After start-up at 7 am the outlet temperature of the BHXs is about 13 °C. Due to the cooling load of the air conditioning system it slowly increases during the day. The temperature level demanded by the cooling ceilings and the air cooler is roughly 18 °C. A switch between the BHXs is conducted as soon as the cold water temperature supplied by the BHX exceeds this temperature level. On hot days more than 10 switches are conducted. In this way the area of heat transfer is increased while electricity demand of the pumps is kept as low as possible.

Fig. 12 (left) shows the overall amount of energy transferred to the soil through both BHXs during each of the investigated months. To judge on the overall efficiency of the BHXs, a Monthly Performance Factor MPF as well as a Seasonal Performance Factor SPF are presented. The quantities relate the transferred energy as heat with the necessary electricity to drive the pumps for the respective period:

$$\mathrm{MPF} = \frac{\int_{\mathrm{m}} \dot{Q}_{\mathrm{BHX}} \mathrm{d}t}{\int_{\mathrm{m}} P_{\mathrm{el}} \mathrm{d}t} \quad \mathrm{SPF} = \frac{\int_{\mathrm{p}} \dot{Q}_{\mathrm{BHX}} \mathrm{d}t}{\int_{\mathrm{p}} P_{\mathrm{el}} \mathrm{d}t} \tag{6}$$

The overall high efficiency is based on the application of variable speed pumps, the choice of adequate pipe diameters, a sufficient number of BHXs and the chosen operation strategy. During July by far the most energy as heat was transferred to the soil, which is a result of the occurring highest cooling loads. Despite the increased soil temperature, the MPF also exhibited the highest value during July (MPF = 212 ± 18). Due to the mentioned control strategy, the denominator in Eq. (6) stays fairly constant during the investigated period. However, the numerator changes according to the average power as heat transferred at the BHXs. The average transferred power (indicated by the diamond symbols in Fig. 12) shows the same behaviour as the MPF values, underlining the given explanation. Evaluating the performance for the whole season, a Seasonal Performance Factor of SPF = 192 ± 16 is achieved, indicating a highly efficient cooling process.

The applicability of the presented system to other locations strongly depends on the prevalent soil and climate conditions. The results presented here are expectable for similar climate conditions as presented in Fig. 5, Table 7 gives a brief overview of the

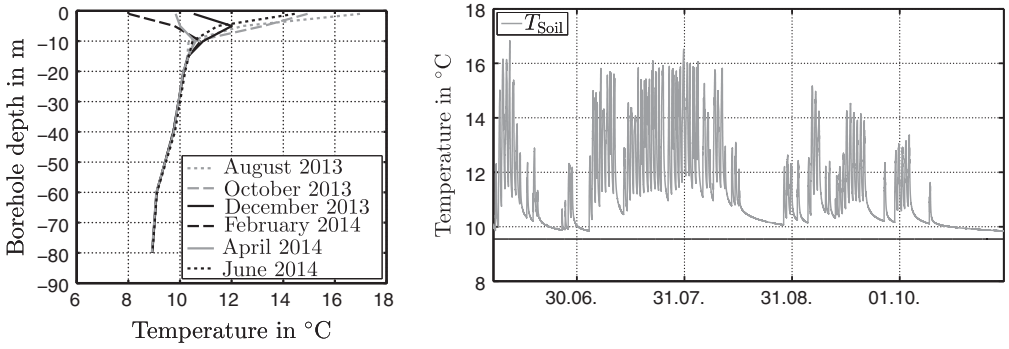

Fig. 10. Undisturbed soil temperature BHX 2 (left) and temperature below 15 m during the cooling period for BHX 3 (right).

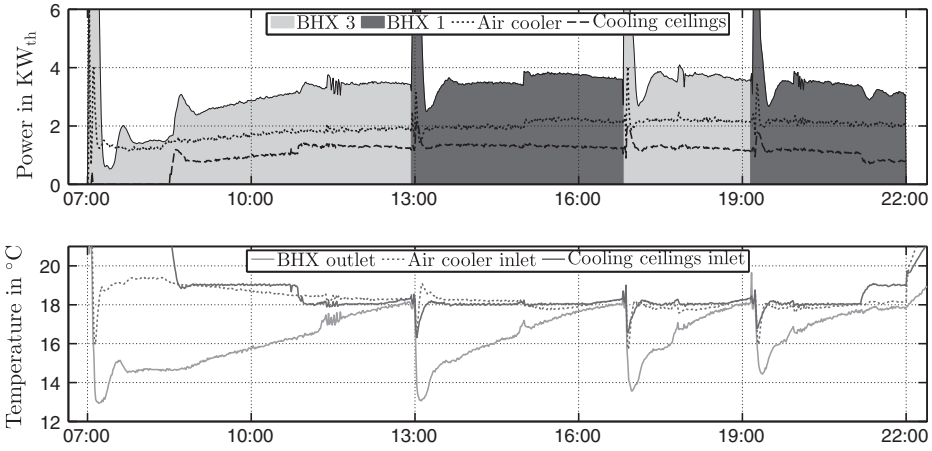

Fig. 11. Cooling supply and demand (upper graph) and respective temperature levels (lower graph).

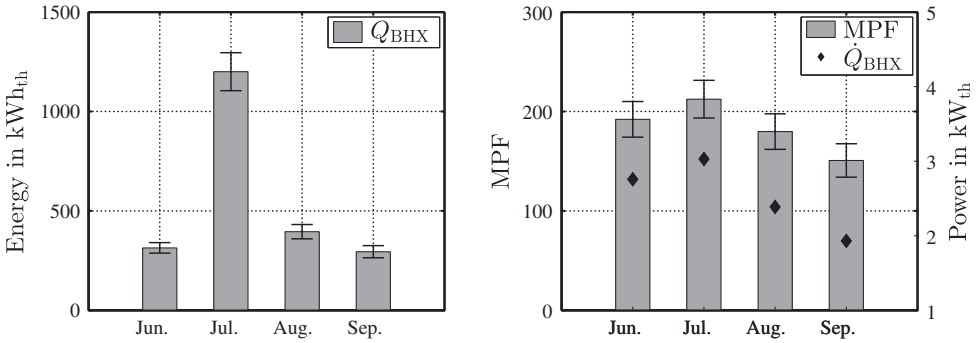

Fig. 12. Energy transferred to the soil (left) and Monthly Performance Factor of the BHXs (right).

influence of changing ambient conditions. For higher occurring latent loads, a two stage desiccant system might be required. As indicated above, the soil temperature below 15 m usually equals the mean yearly temperature which therefore is a good indicator for the applicability of direct geothermal cooling. The high cold water temperature level of the presented system (>17 °C) enables the possibility to use geothermal cooling in an efficient way. The system is planned to work in temperate climates with mean yearly temperatures below 13 °C and applicable latent loads. However, the exact soil conditions of the respective location need to be taken into account to size the system.

4. Conclusions

If climate and soil conditions are suitable, the combined operation of an open cycle desiccant assisted air conditioning system and borehole heat exchangers can significantly decrease the electricity demand required for air conditioning. The presented hybrid system achieves an electric energy efficiency ratio of 6.63 during the investigated period. Primary energy savings can be achieved even if comparatively inefficient heat conversion processes are used to generate the thermal energy required for regeneration of the desiccant wheel. Given the local soil conditions of the test facility, borehole heat exchangers offer a highly efficient possibility for renewable cooling, exhibiting a seasonal performance factor of SPF = 192. If borehole heat exchangers are used in combination with a heat pump during the winter period, the system offers an attractive possibility for a full air conditioning system realizing cooling, heating, enthalpy recovery and dehumidification. However, a detailed economic evaluation of the system is required to finally judge on its chances for a broad application.

Acknowledgement

This work is being conducted in the frame of a project funded by the Federal Ministry for Economic Affairs and Energy (www.bmwi.de), cf. project funding reference number 03ET1065A.

References

[1] IEA – International Energy Agency. Energy efficiency market report 2015. Paris: OECD/IEA; 2015.
[2] Isaac M, Van Vuuren DP. Modeling global residential sector energy demand for heating and air conditioning in the context of climate change. Energy Policy 2009;37:507–21.
[3] Hitchin R, Pout C, Riviere P. Assessing the market for air conditioning systems in European buildings. Energy Build 2013;58:355–62.
[4] Jani DB, Mishra M, Sahoo PK. Solid desiccant air conditioning – a state of the art review. Renew Sustain Energy Rev 2016;60:1451–69.
[5] Angrisani G, Capozzoli A, Minichiello F, Roselli C, Sasso M. Desiccant wheel regenerated by thermal energy from a microgenerator: experimental assessment of the performances. Appl Energy 2011;88:1354–65.
[6] Eicker U, Schürger U, Köhler M, Ge T, Dai Y, Li H, et al. Experimental investigations on desiccant wheels. Appl Therm Eng 2012;42:71–80.
[7] Al-Alili A, Hwang Y, Radermacher R. Performance of a desiccant wheel cycle utilizing new zeolite material: experimental investigation. Energy 2015;81:137–45.
[8] Ruivo CR, Angrisani G, Minichiello F. Influence of the rotation speed on the effectiveness parameters of a desiccant wheel: an assessment using experimental data and manufacturer software. Renew Energy 2015;76:484–93.
[9] Ruivo CR, Costa JJ, Figueiredo AR. Parametric study of the cyclic behaviour of a hygroscopic matrix in a desiccant airflow system. Heat Mass Transf 2011;47:1101–12.
[10] Yamaguchi S, Saito K. Numerical and experimental performance analysis of rotary desiccant wheels. Int J Heat Mass Transf 2013;60:51–60.
[11] Ge TS, Ziegler F, Wang RZ. A mathematical model for predicting the performance of a compound desiccant wheel (a model of compound desiccant wheel). Appl Therm Eng 2010;30:1005–115.
[12] Fu XF, Zhang LZ, Xu JC, Cai RR. A dual-scale analysis of a desiccant wheel with a novel organic-inorganic hybrid adsorbent for energy recovery. Appl Energy 2016;163:167–79.
[13] La D, Dai YJ, Li Y, Wang RZ, Ge TS. Technical development of rotary desiccant dehumidification and air conditioning: a review. Renew Sustain Energy Rev 2010;14:130–47.
[14] Ge TS, Dai YJ, Wang RZ. Review on solar powered rotary desiccant wheel cooling system. Renew Sustain Energy Rev 2014;39:476–97.
[15] Rafique MM, Gandhidasan P, Rehman S, Al-Hadhrami LM. A review on desiccant based evaporative cooling systems. Renew Sustain Energy Rev 2015;45:145–59.
[16] Sultan M, El-Sharkawy II, Miyazaki T, Saha BB, Koyoma S. An overview of solid desiccant dehumidification and air conditioning. Renew Sustain Energy Rev 2015;46:16–29.
[17] Kojok F, Fardoun F, Younes R. Hybrid cooling systems: a review and an optimized selection scheme. Renew Sustain Energy Rev 2016;65:57–80.
[18] Al-Alili A, Hwang Y, Radermacher R, Kubo I. A high efficiency solar air conditioner using concentrating photovoltaic/thermal collectors. Appl Energy 2012;93:138–47.
[19] Fong KF, Lee CK, Chow TT, Fong AML. Investigation on solar hybrid desiccant cooling system for commercial premises with high latent cooling load in subtropical Hong Kong. Appl Therm Eng 2011;31:3393–401.
[20] Wrobel J, Walter P Sanabria, Schmitz G. Performance of a solar assisted air conditioning system at different locations. Sol Energy 2013;92:69–83.
[21] Mazzei P, Minichiello D, Palma D. Desiccant HVAC systems for commercial buildings. Appl Therm Eng 2002;22:545–60.
[22] Angrisani G, Roselli C, Sasso M. Experimental assessment of the energy performance of a hybrid desiccant cooling system and comparison with other air-conditioning technologies. Appl Energy 2015;138:533–45.
[23] Dhar PL, Singh SK. Studies on solid desiccant based hybrid air conditioning systems. Appl Therm Eng 2001;21:119–34.
[24] Fong KF, Lee CK, Chow TT, Lin Z, Chan LS. Solar hybrid air-conditioning system for high temperature cooling in subtropical city. Renew Energy 2010;35:2439–51.
[25] Speerforck A, Schmitz G. Integration of an adsorption chiller in an open cycle desiccant assisted air conditioning system. Sci Technol Built Environ 2015;21:375–83.
[26] El-Agouz SA, Kabeel AE. Performance of desiccant air conditioning system with geothermal energy under different climatic conditions. Energy Convers Manage 2014;88:464–75.
[27] Enteria N, Yoshino H, Takaki R, Mochida A. Case analysis of utilizing alternative energy sources and technologies for the single family detached house. Sol Energy 2014;105:243–63.
[28] Khalajzadeh V, Famahini-Farahani M, Heidarinejad G. A novel integrated system of ground heat exchanger and indirect evaporative cooler. Energy Build 2012;49:604–10.
[29] Angrisani G, Diglio G, Sasso M, Calise F, d'Accadia M Dentice. Design of a novel geothermal heating and cooling system: energy and economic analysis. Energy Convers Manage 2016;108:144–59.

[30] Schmitz G, Casas W. Experiences with a gas driven, desiccant assisted air conditioning system with geothermal energy for an office building. Energy Build 2005;37:493–501.
[31] Wrobel J, Schmitz G. Geothermal- and solar assisted air conditioning system. In: International refrigeration and air conditioning conference, paper 2372; 2012.
[32] Niu JL, Zhang LZ, Zuo HG. Energy savings potential of chilled ceiling combined with desiccant cooling in hot and humid climates. Energy Build 2002;34:487–95.
[33] Slayzak SJ, Ryan JP. Desiccant dehumidification wheel test guide. NREL technical report, NREL/TP-550-56131; 2000.
[34] DIN EN ISO 5167-2. Measurement of fluid flow by means of pressure differential devices inserted in circular cross-section conduits running full – part 2: orifice plates; 2004.
[35] Chunovkina A. Measurement error, measurement uncertainty, and measurand uncertainty. Meas Tech 2000;43:581–6.
[36] Wrobel J, Morgenstern P, Schmitz G. Modeling and experimental validation of the desiccant wheel in a hybrid desiccant air conditioning system. Appl Therm Eng 2013;51:1082–91.
[37] DIN EN ISO 15251. Indoor environmental input parameters for design and assessment of energy performance of buildings addressing indoor air quality, thermal environment, lighting and acoustics; 2012.
[38] Napolitano A, Wolfram S, Thür A, Finocchiaro P, Nocke B. Monitoring procedure for solar cooling systems – a joint technical report of subtask A and B; 2011.
[39] DIN V 18599-1. Energy efficiency of buildings – calculation of the net, final and primary energy demand for heating, cooling, ventilation, domestic hot water and lighting – part 1: general balancing procedures, terms and definitions, zoning and evaluation of energy sources; 2013.
[40] Eicker U, Vorschulze C. Potential of geothermal heat exchangers for office building climatisation. Renew Energy 2009;34:1126–33.